Electronic Supplementary Material (ESI) for Sustainable Energy & Fuels.

Supporting Information

Construction of Sol-gel derived Ternary CuZn/FeO_x Nanostructure for Catalytic Transfer Hydrogenation of Furfural

Tao Wang, Yuan Cheng, Hongyu Niu, Shaojie Li, Jingjie Luo,* Changhai Liang*

Laboratory of Advanced Materials & Catalytic Engineering (AMCE), School of Chemical Engineering, Dalian University of Technology, Panjin 124221, China

*Corresponding author. Tel/Fax: +86-411-84986353;

E-mail: jingjie.luo@dlut.edu.cn (J. Luo) & changhai@dlut.edu.cn (C. Liang)

Table contents

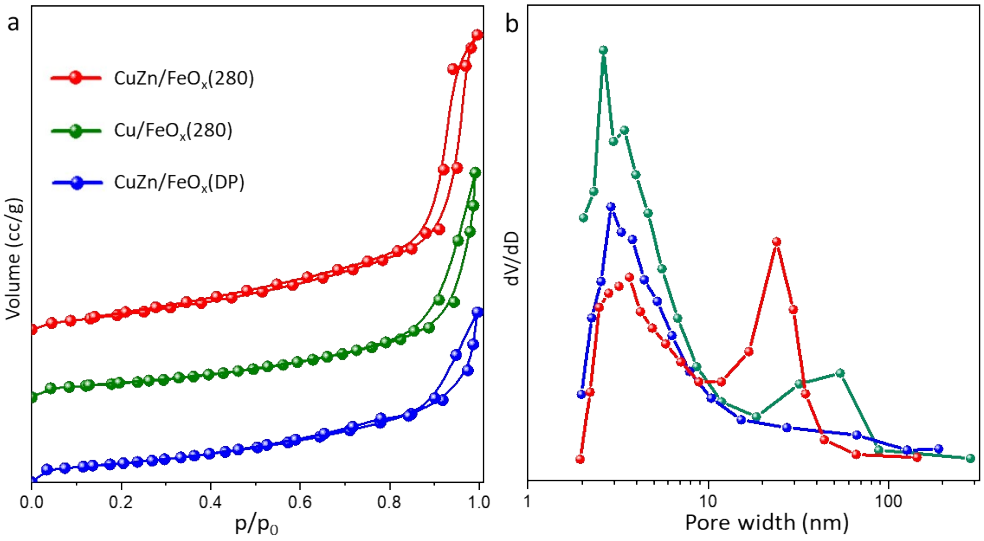

Figure S1. N_2 adsorption–desorption isotherms and pore size distributions of Cu/FeO_x(280) and CuZn/FeO_x(280) catalysts by sol-gel and CuZn/FeO_x(DP) by deposition-precipitation.

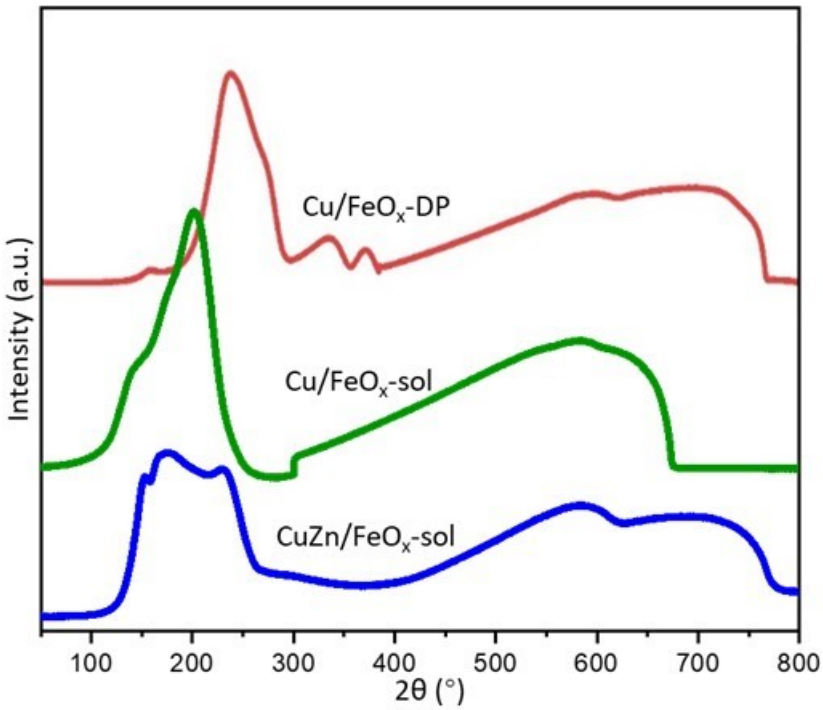

Figure S2. H_2-TPR profiles of precursors after calcined at 500 °C without further thermal reduction: sol-gel derived Cu/FeO_x-sol and $CuZn/FeO_x$-sol precursors; DP derived Cu/FeO_x-DP precursor.

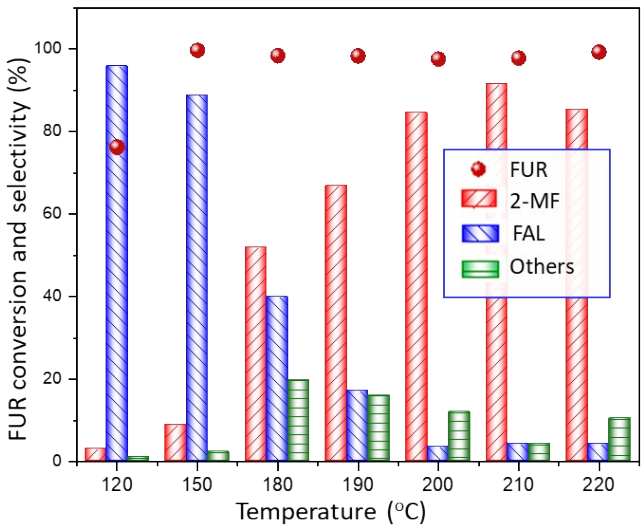

Figure S3. Catalytic performance of CuZn/FeO_x(280) for the CTH process of FUR as a function of reaction temperature. Reaction conditions: molar ratio of furfural/isopropanol = 0.02, 200 mg of catalyst, 4 h, 0.1 MPa N_2. FUR: furfural, 2-MF: 2-methylfuran, FAL: furfuryl alcohol. Other products including condensation and coupling products with minor amount of γ-valerolactone.

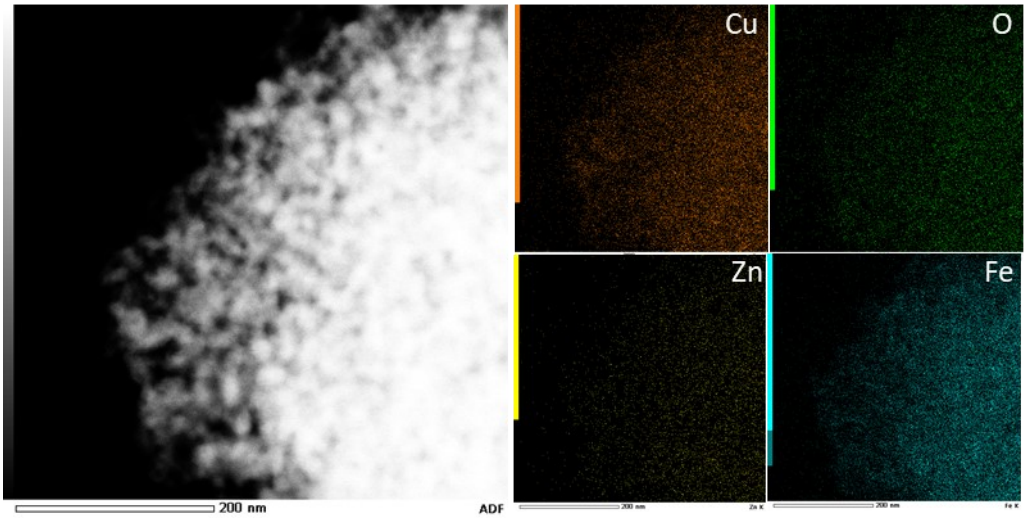

Figure S4. HAADF-STEM elemental mappings of CuZn/FeO_x(250).

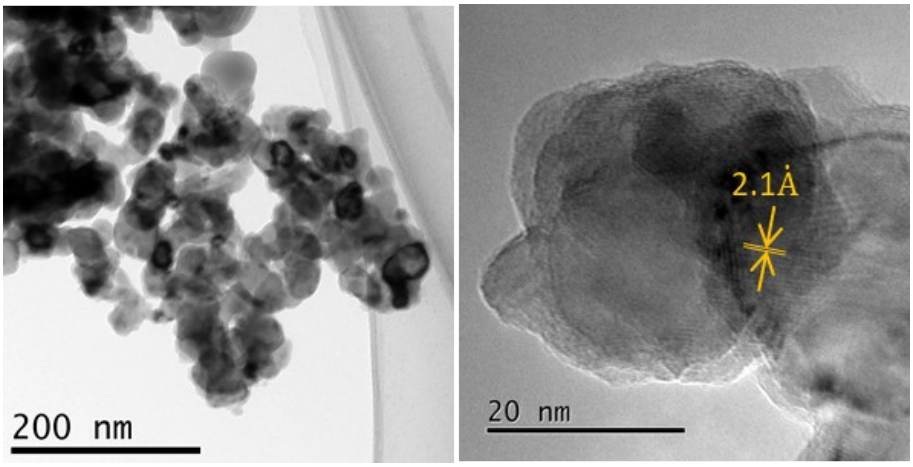

Figure S5. TEM images of CuZn/FeO_x(280) catalyst.

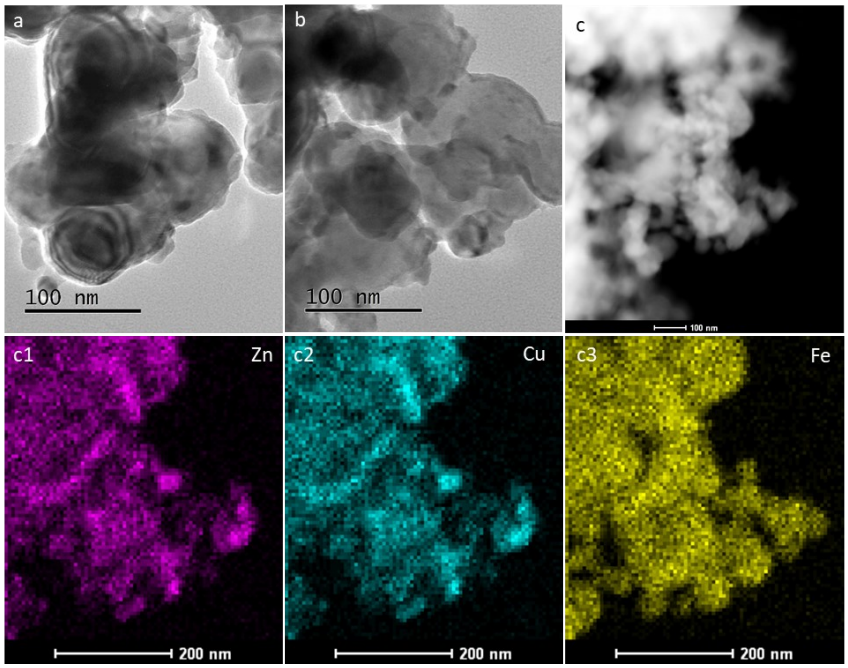

Figure S6. TEM images and HAADF-STEM elemental mappings of $CuZn/FeO_x(350)$.

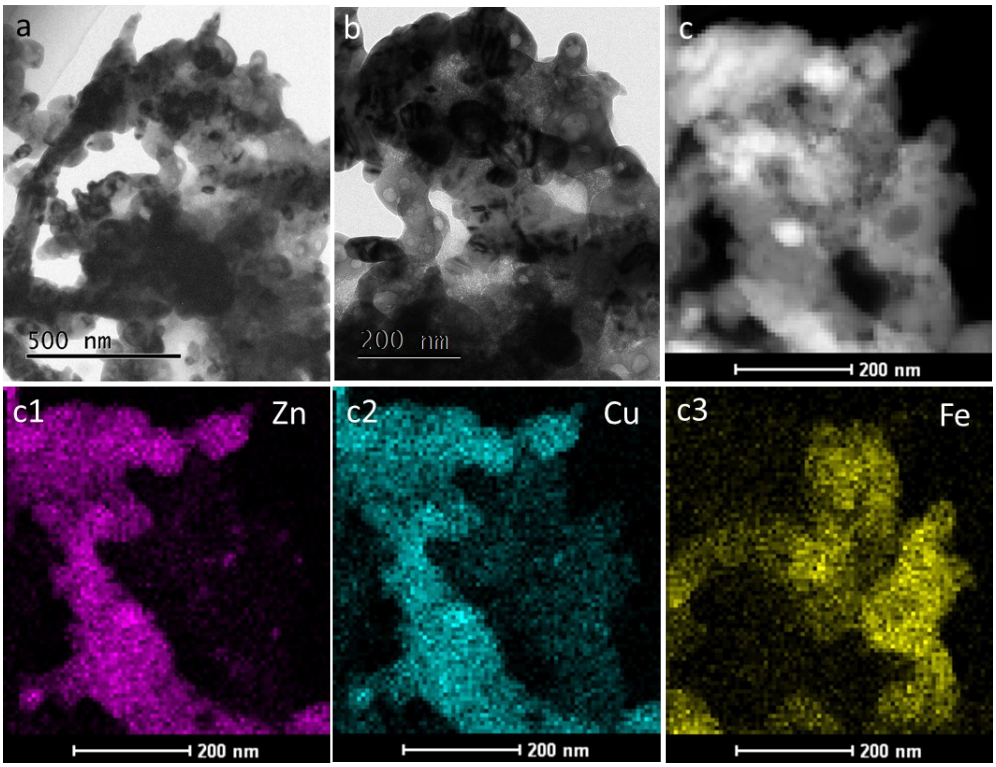

Figure S7. TEM images and HAADF-STEM elemental mappings of CuZn/FeO_x(DP) synthesized by deposition-precipitation.

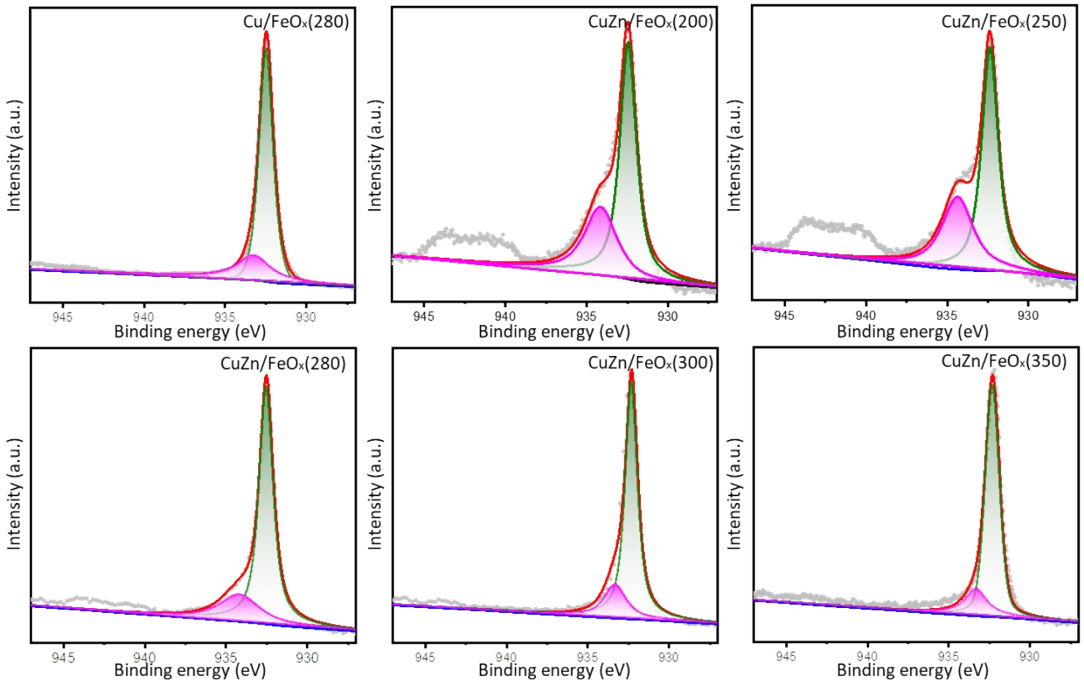

Figure S8. XPS spectra of Cu 2*p* core level of the Cu/FeO_x and CuZn/FeO_x catalysts.

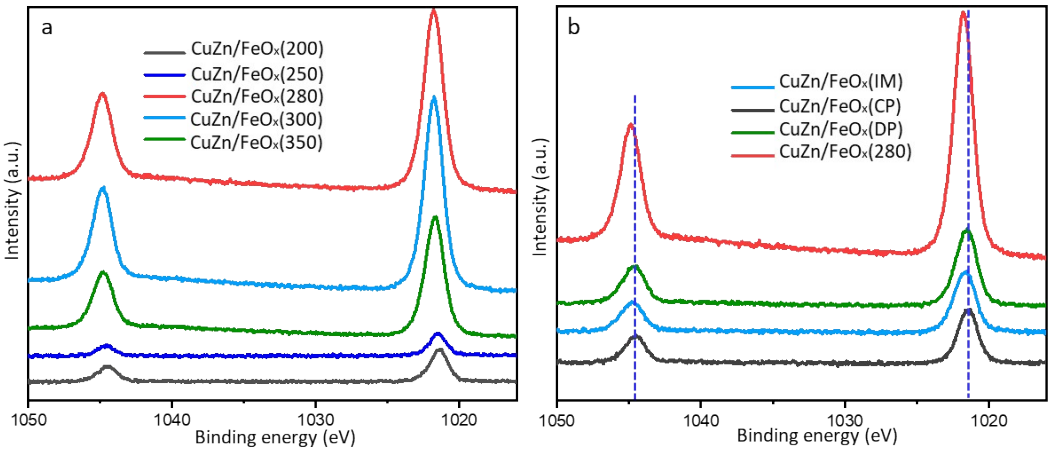

Figure S9. XPS spectra of Zn 2*p* core level of (a) Cu/FeO_x and CuZn/FeO_x by sol-gel methods, and (b) CuZn/FeO_x catalysts by conventional methods pre-reduced at 280 °C.

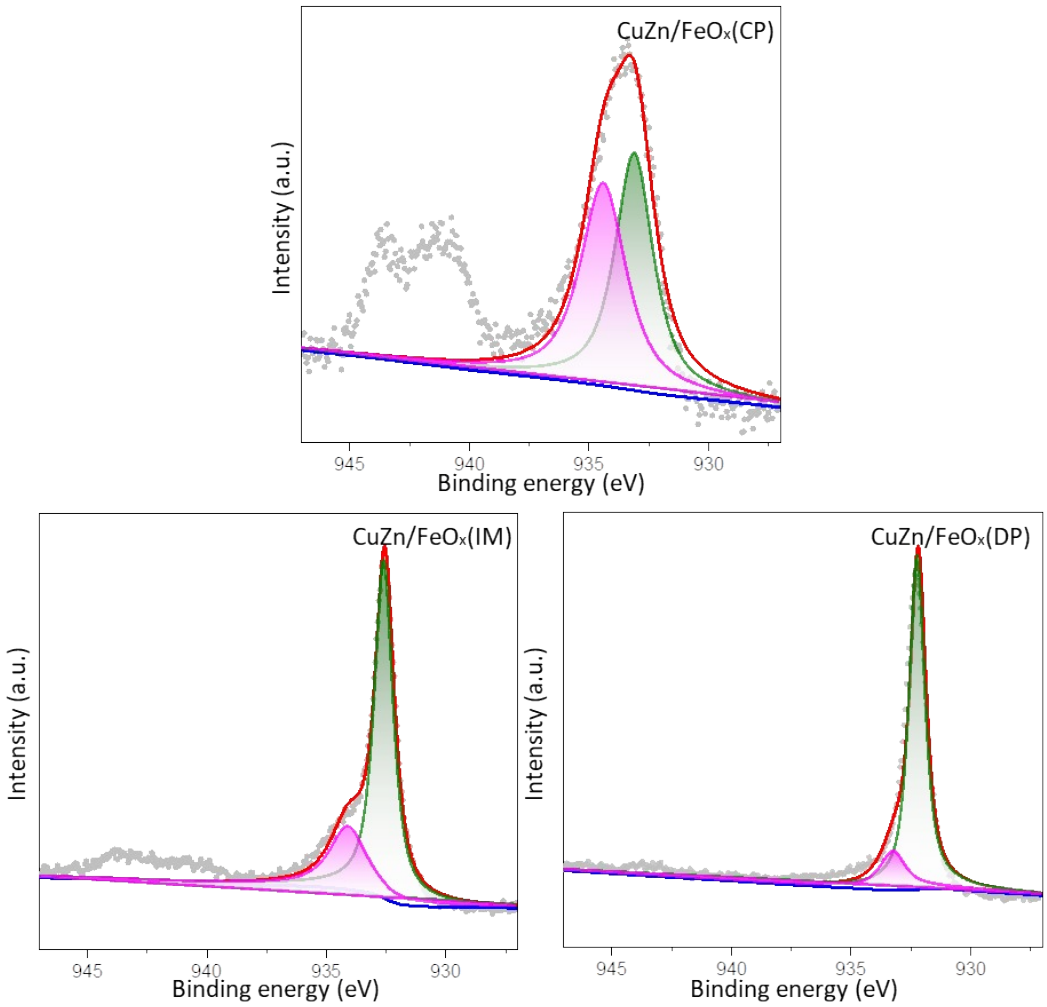

Figure S10. XPS spectra of Cu 2*p* core level of the $CuZn/FeO_x$ catalysts by different methods.

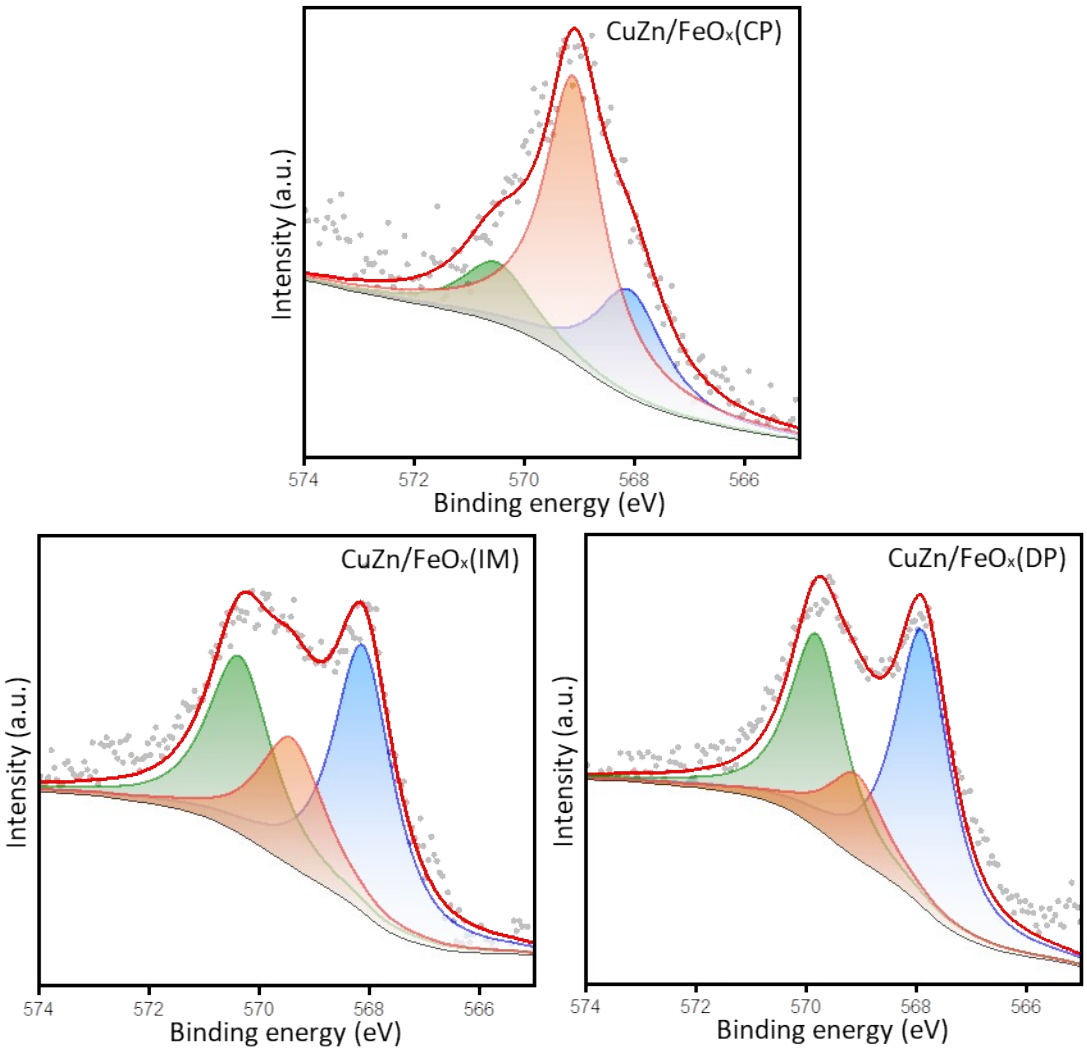

Figure S11. Cu LMM XPS spectra of the CuZn/FeO_x catalysts by different methods.

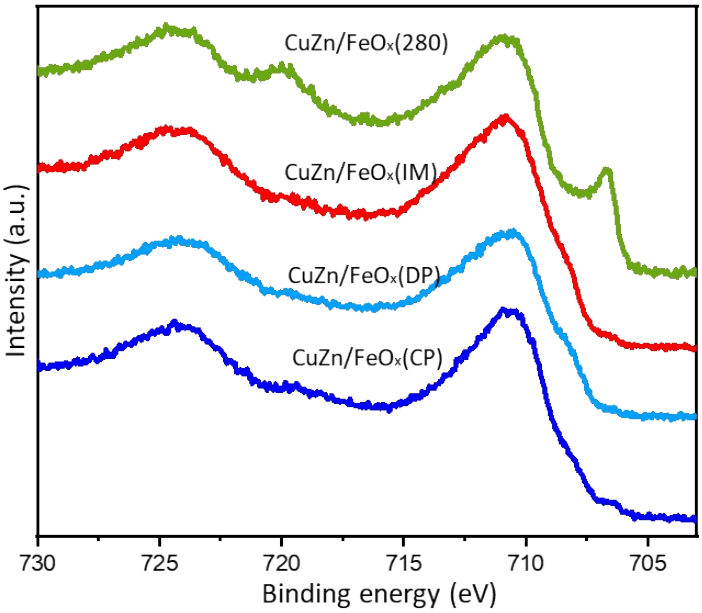

Figure S12. XPS spectra of Fe 2*p* core level of the CuZn/FeO_x catalysts by different methods.

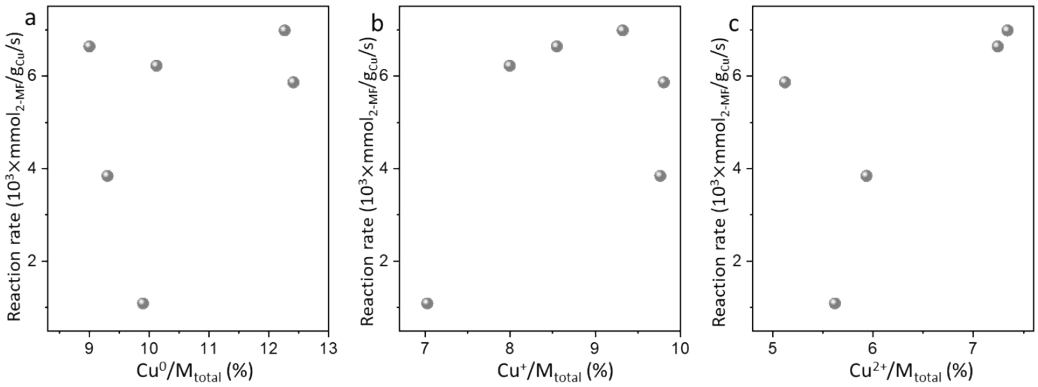

Figure S13. The reaction rates by different catalysts changed with the (a) surface percentage of Cu^0, (b) percentage of Cu^+, and (c) percentage of Cu^{2+}. There was no clear tendency between the reaction rates and the percentages of surface copper species. The Cu/M_{total} was standardized by the atomic ratio of copper species in the total metal elements (Cu+Fe+Zn).

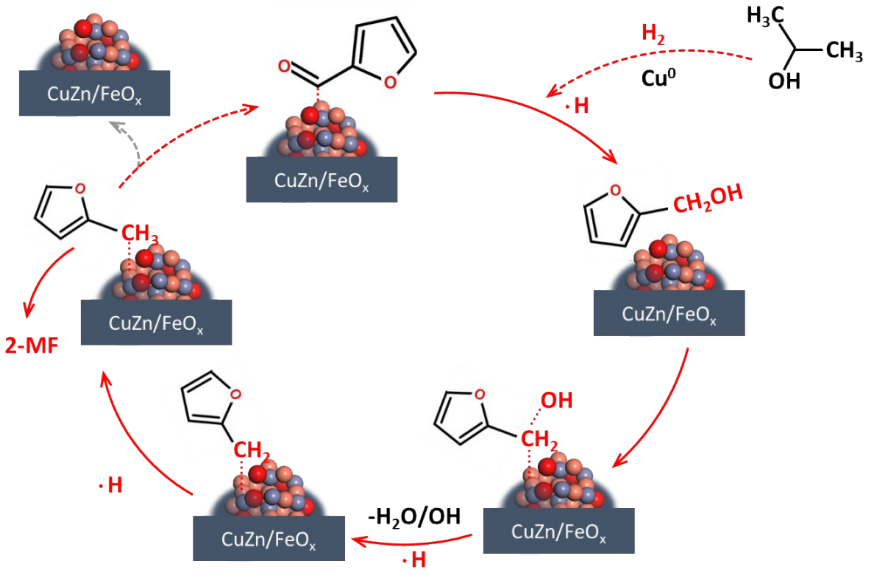

Figure S14. The CTH reaction mechanism of FUR using CuZn/FeO_x catalysts. The origin ball, purple ball, and red ball suggested the Cu, Zn and O atoms.

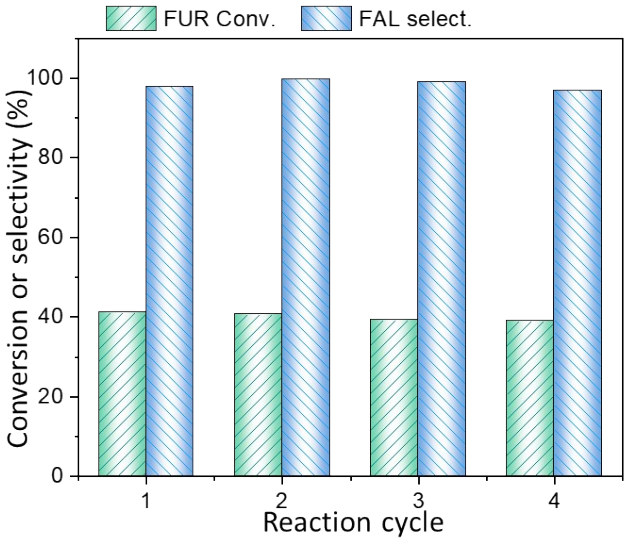

Figure S15. FUR conversion and product distribution during cycle reaction by $CuZn/FeO_x(280)$. Reaction condition: molar ratio of furfural/isopropanol = 0.02, 100 mg of catalyst, 180 °C for 4 h, 0.1 MPa N_2. FUR: furfural, FAL: furfuryl alcohol.

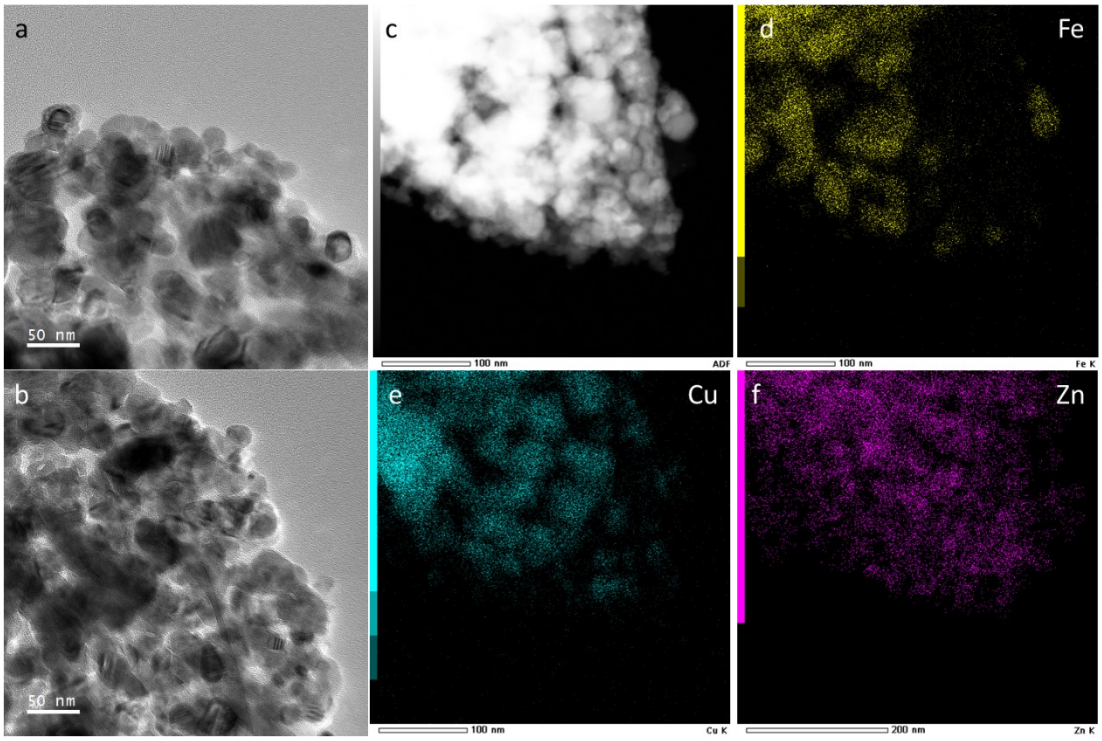

Figure S16. TEM images and the HAADF-STEM elemental mappings of CuZn/FeO_x(280) after reaction.

Table S1. Structure and surface information of Cu catalysts according to XRD and XPS data.

Sample	Method	Pre-reduction T (°C)	$d_{Cu(111)}$[a]	Surface composition (%)		
				Cu^0	$(Cu^0+Cu^+)/Cu^{2+}$	Cu^+/Cu^0
Cu/FeO_x(280)	Sol-gel	280	18.4	37.2	3.51	1.05
$CuZn/FeO_x$(200)		200	8.3	36.3	2.46	0.95
$CuZn/FeO_x$(250)		250	9.6	42.4	3.45	0.76
$CuZn/FeO_x$(280)		280	11.6	45.9	4.63	0.79
$CuZn/FeO_x$(300)		300	15.7	45.4	4.35	0.79
$CuZn/FeO_x$(350)		350	26.6	43.9	6.65	0.71
$CuZn/FeO_x$(CP)	Co-precipitation	280	18.3	24.8	0.63	0.56
$CuZn/FeO_x$(DP)	Deposition-precipitation		21.7	48.7	4.84	0.70
$CuZn/FeO_x$(IM)	Impregnation		19.8	44.4	3.19	0.72

[a] Average sizes of Cu particles estimated by Scherrer equation based on the peak width at half height of Cu (111) diffraction peaks.

Table S2. Surface acid sites in terms of the NH_3 desorption amount based on the NH_3-TPD profiles.

Sample	NH_3 desorption (NH_3 mmol/g)			
	Weak	Medium	Strong	Total
$Cu/FeO_x(280)$	0.017	0.008	0.005	0.030
$CuZn/FeO_x(250)$	0.019	0.010	0.030	0.059
$CuZn/FeO_x(280)$	0.014	0.011	0.011	0.036
$CuZn/FeO_x(300)$	0.013	0.012	0.004	0.029
$CuZn/FeO_x(350)$	0.013	0.009	0.005	0.027

Table S3. Comparison of specific rates in the current work and the reported literature.

Catalyst	T (°C)	2-MF yield	Specific rate ($\mu mol_{2-MF}/g_M/s$)	Ref.
CuZn/FeO_x(280)	190	66.8	6.2	This work
CuZn/FeO_x(280)	210	92.0	8.6	This work
Cu/FeO_x-C5H	220	80.5	2.2	[1]
NiCuAl	200	41.1	1.5	[2]
10Cu3Pd/ZrO_2	220	61.9	0.4	[3]
$Cu_{2.5}$Zn−Al-600	180	72.0	2.1	[4]
5Cu3Re/Al_2O_3	220	94.0	3.4	[5]
10%Ni-10%Cu	210	73.6	4.6	[6]
Cu/SiO_2-HT	220	90.0	12.8[a]	[7]
Ru/C	180	61.0	0.3	[8]
Ru_4/$NiFe_2O_4$	200	79.0	0.8	[9]

[a] Initial N_2 pressure was kept at 2.1 MPa.

References

[1] J.J. Luo, Y. Cheng, H.Y. Niu, T. Wang, C.H. Liang, J Catal, 413 (2022) 575-587.

[2] M. Kalong, P. Hongmanorom, S. Ratchahat, W. Koo-amornpattana, K. Faungnawakij, S. Assabumrungrat, A. Srifa, S. Kawi, Fuel Process Technol, 214 (2021) 106721.

[3] X. Chang, A.F. Liu, B. Cai, J.Y. Luo, H. Pan, Y.B. Huang, Chemsuschem, 9 (2016) 3330-3337.

[4] H.Y. Niu, J.J. Luo, C. Li, B.W. Wang, C.H. Liang, Industrial & Engineering Chemistry Research, 58 (2019) 6298-6308.

[5] K. Zhou, J.X. Chen, Y.J. Cheng, Z.T. Chen, S.M. Kang, Z.D. Cai, Y.J. Xu, J.J. Wei, ACS Sustainable Chemistry & Engineering, 8 (2020) 16624-16636.

[6] Z. Fu, Z. Wang, W. Lin, W. Song, S. Li, Applied Catalysis A: General, 547 (2017) 248-255.

[7] B. Li, L. Li, H. Sun, C. Zhao, ACS Sustainable Chemistry & Engineering, 6 (2018) 12096-12103.

[8] M.J. Gilkey, P. Panagiotopoulou, A.V. Mironenko, G.R. Jenness, D.G. Vlachos, B.J. Xu, Acs Catal, 5 (2015) 3988-3994.

[9] B. Wang, C. Li, B. He, J. Qi, C. Liang, Journal of Energy Chemistry, 26 (2017) 799-807.